Ice Sheet System Model

ISSM Capabilities

Eric LAROUR[1], Eric RIGNOT[1,3], Mathieu MORLIGHEM[1,2], Hélène SEROUSSI[1,2] Chris BORSTAD[1], Feras HABBAL[1,3], Daria HALKIDES[1,4], Behnaz KHAKBAZ[1], John SCHIERMEIER[1], Nicole SCHLEGEL[1]

[1] Jet Propulsion Laboratory - California Institute of Technology

[2] Laboratoire MSSMat, École Centrale Paris, France

[3] University of California, Irvine

[4] Joint Institute for Regional Earth System Science & Engineering, UCLA

 ©Copyright 2011. All rights reserved

Outline

Introduction

History of ISSM

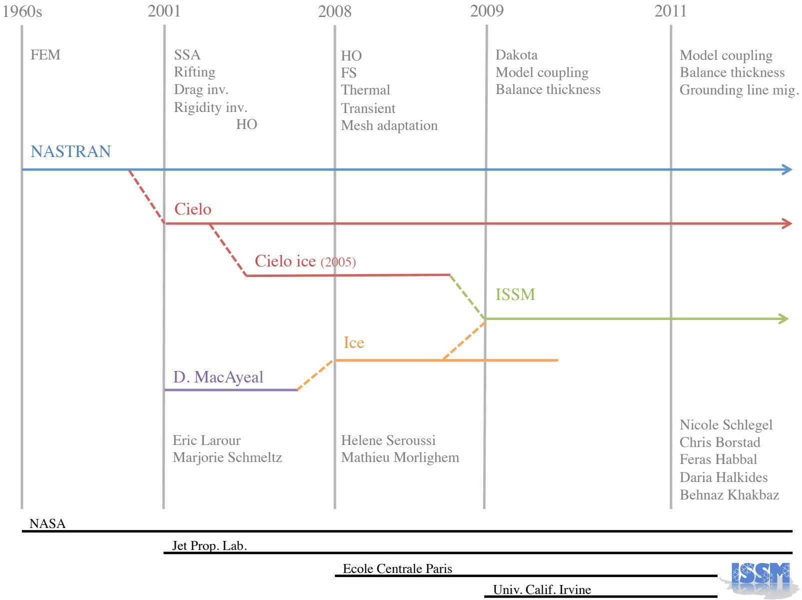

Diagnostic models of ice flow

Solve mechanical stress-equilibrium for the entire ice sheet/ice shelf. Can be done in 2D (SSA) or 3D (SIA, Higher-order, Full-Stokes). Material is isotropic nonlinear (Glen's law) in the creep regime of deformation.

$$\nabla \bullet \vec{V} = 0$$

$$\rho \frac{d\vec{V}}{dt} = \nabla \bullet \sigma + \rho \vec{g}$$

$$\sigma_{ij}' = 2\eta \dot{\varepsilon}_{ij}$$

$$\eta = \frac{1}{2} A(\theta)^{\frac{-1}{n}} \left(\dot{\varepsilon} + \dot{\varepsilon}_0 \right)^{\frac{(1-n)}{n}}$$

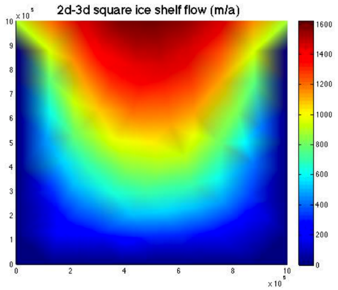

Inversion

Rely on surface velocities (InSAR) to inver unknown parameters in the ice flow equations, such as viscosity, ice rigidity or basal drag.

$$J' = \iint_S \frac{1}{2}\left\{(u - u_{obs})^2 + (v - v_{obs})^2\right\} dxdy +$$

$$\iint_S \lambda(x,y)\left\{\frac{\partial}{\partial x}\left(2\nu H\left(2\frac{\partial u}{\partial x} + \frac{\partial v}{\partial y}\right)\right) + \frac{\partial}{\partial y}\left(\nu H\left(\frac{\partial u}{\partial y} + \frac{\partial v}{\partial x}\right)\right) - \rho g H\frac{\partial z_s}{\partial x} - \beta^2 u\right\} dxdy +$$

$$\iint_S \mu(x,y)\left\{\frac{\partial}{\partial y}\left(2\nu H\left(2\frac{\partial v}{\partial y} + \frac{\partial u}{\partial x}\right)\right) + \frac{\partial}{\partial x}\left(\nu H\left(\frac{\partial u}{\partial y} + \frac{\partial v}{\partial x}\right)\right) - \rho g H\frac{\partial z_s}{\partial y} - \beta^2 v\right\} dxdy$$

$$\frac{dJ'}{d\beta} = -2\iint_S \{\lambda u + \mu v\}\beta\delta\beta \, dxdy$$

Inversion

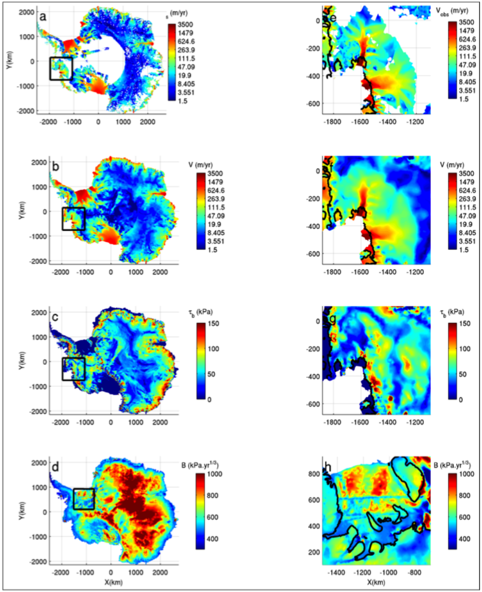
a
b
c
d
e
g
h
Y(km)
X(km)
(m/yr)
V_{obs} (m/yr)
V (m/yr)
3500
1479
624.6
263.9
111.5
47.09
19.9
8.405
3.551
1.5
τ_b (kPa)
150
100
50
0
B (kPa.yr$^{1/3}$)
1000
800
600
400
2000
1000
0
-1000
-2000
-200
-400
-600
-1800
-1600
-1400
-1200
800
600
400
200
-1400
-1200
-1000
-800

Parallel computing

- ISSM can run on any platform (multi-core desktop), shared or distributed cluster
- C++ implementation of computational core using MPICH and PETSc libraries + array of parallel libraries for partitioning, iterative and direct solvers
- Multi-threading of pre and post-processing modules to increase speed significantly

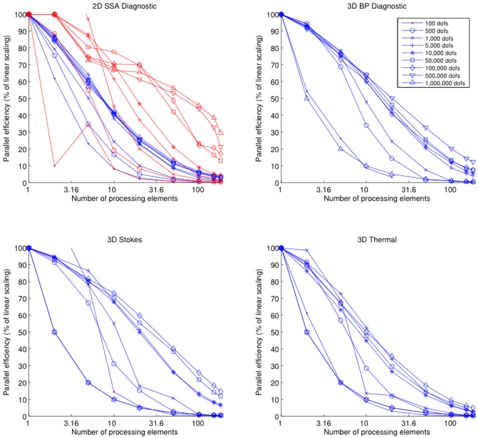

Rifting/Faulting

ISSM can account for the presence of rifts and faults in an ice shelf by carrying out a steady-state computation of the contact within the rifts/faults.

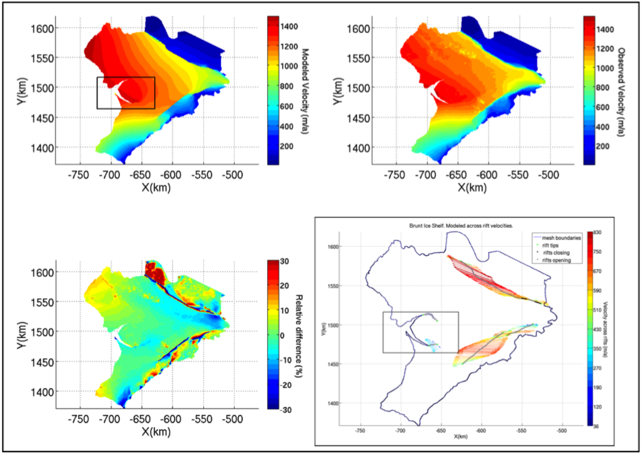

Rifting/Faulting

- Rifting and faulting account for contact stresses and the presence of melange
- This is not an initiation or propagation capability
- Relies on penalty methods to enforce contact conditions between flanks of rifts
- Relies on diagnostic model to compute stresses across ice shelf
  - This is not an LEFM capability. It assumes the entire ice shelf is creeping, and there is no inclusion of elastic stresses

Higher-order and Full-Stokes modeling

- ISSM relies on the the 2D SSA to capture longitudinal stresses, 3D Blatter/Pattyn to capture vertical shear stresses and full-Stokes equations to capture all stresses within the ice sheet
- Activation of all three formulations is seamless, relying on almost the same model setup $\rightarrow$ experimentation is easy
- Coupled with parallel computing and anisotropic meshing, higher-order modeling at the continental scale is achievable with reasonable resolutions

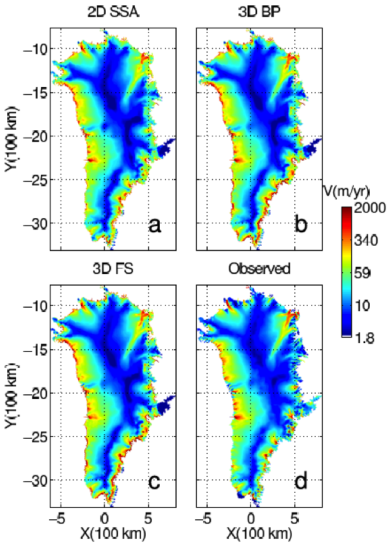

Figure 8. Modeled surface velocity (in m/yr) (using inverted basal drag coefficient) for the 2D Shelfy-Stream model (a), the 3D Blatter/Pattyn model (b) and the 3D full-Stokes model (c). d) Observed InSAR surface ities (in m/yr) of the Greenland Ice Sheet.

Anisotropic adaptation

- Adapt mesh according to a metric, such as surface velocity
- Static capability, not transient adaptation
- Relies on a rewrite of the BAMG anisotropic mesher [Hecht, 2006]

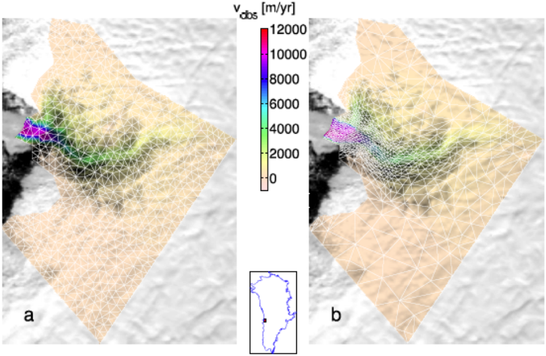

Figure 2. Anisotropic adaptive mesh of Jakobshavn Isbræ, West Greenland. a) InSAR surface velocity interpolated on a uniform mesh, b) InSAR surface velocity from *Rignot* [2008] interpolated on adapted mesh (in white). Both meshes comprise 1,500 elements.

Prognostic modeling

- Mass transport equations:

$$\frac{\partial H}{\partial t} + \nabla \cdot H\overline{\mathbf{v}} = \dot{M}_s - \dot{M}_b$$

- Update of surface and bed is hydrostatic on ice shelves. For ice sheets, surface is updated assuming the bedrock is fixed
- Mass transport equations are coupled with diagnostic and thermal models to allow for complete transient models to be run (SeaRISE 2011)
- Boundary conditions assume fixed thickness at the ice divide, and free flux of mass at the calving front or the grounded margins
- Calving front dynamics not included yet
- Grounding line dynamics is hydrostatically treated

Thermal modeling

- Thermal model, full-advection and full-diffusion in 3D + viscous heating. Mesh velocity in vertical direction.

$$\frac{\partial T}{\partial t} = (\boldsymbol{w} - \boldsymbol{v}) \cdot \nabla T + \frac{k_{th}}{\rho c} \Delta T + \frac{\Phi}{\rho c}$$

- Boundary conditions:
  - $T = T_s$ at surface
  - At ice/bed interface:

$$k_{th} \nabla T \cdot \boldsymbol{n} = G - \boldsymbol{\tau}_b \cdot \boldsymbol{v}_b$$

- [Holland and Jenkins, 1999] at the ice/ocean interface:

$$k_{th} \nabla T \cdot \boldsymbol{n} = -\rho_w c_p M \gamma \left(T - T_f \right)$$

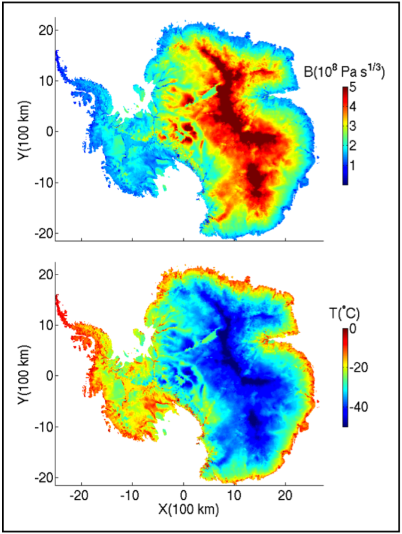

Melting at the ice/bed interface

- Two models for computing melting rates:
  - Linear model where computation of temperatures is updated once for each temperature that goes above pressure melting point
  - Non-linear model where fixed-point scheme is used, where temperatures are updated until all of temperature field is below or at pressure melting point

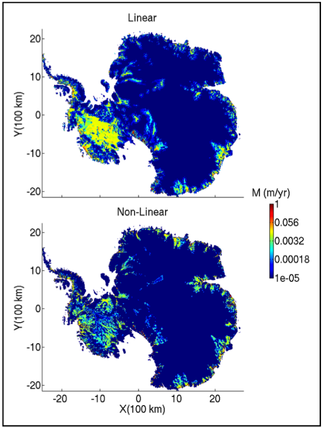

Melting rate is recovered using:

$$S = \frac{\lambda}{\rho_{ice} L}\left(\frac{dT^*}{dz} - \frac{dT}{dz}\right)$$

where T^* is the temperature without pressure melting point constraints and T is the temperature after application of constraints. Non-linear model results in much lower melting rates, even though locations for melting are similar. It is critical to take into account non-linearity of thermal model, at least in steady-state!

Sensitivity analysis

- Sampling and local reliability methods to study the impact of different areas of the mesh
- Sampling of the mesh using Chaco, Scotch and Metis partitioners
- Partition the mesh into equal area sections, which can be then updated for each sample of a Monte-Carlo or local reliability simulation

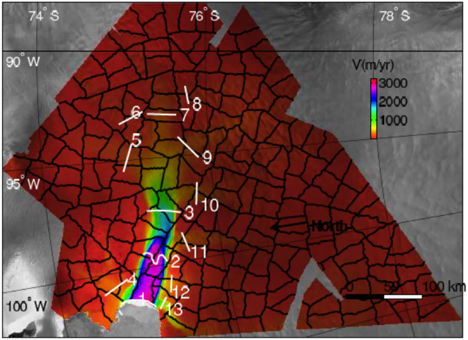

Sensitivity analysis

- Results can then be plotted in histograms for sampling analysis or importance factors for local reliability methods

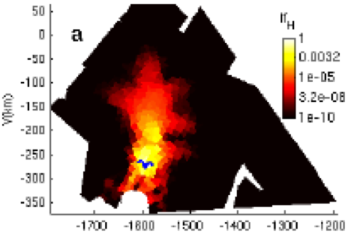

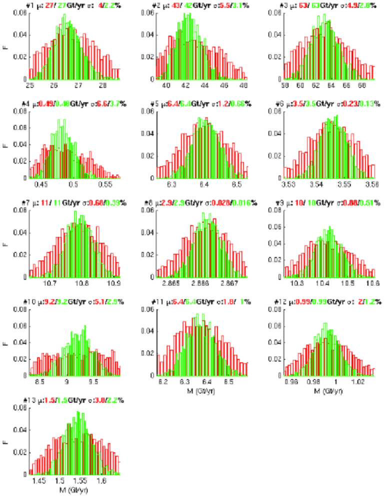

Assimilation of ice thickness (balanced thickness)

- Ice thickness can be optimized to ensure smooth divergence of the flux (thinning rate). Optimization can be constrained (on satellite or airborne tracks where data was measured) or unconstrained

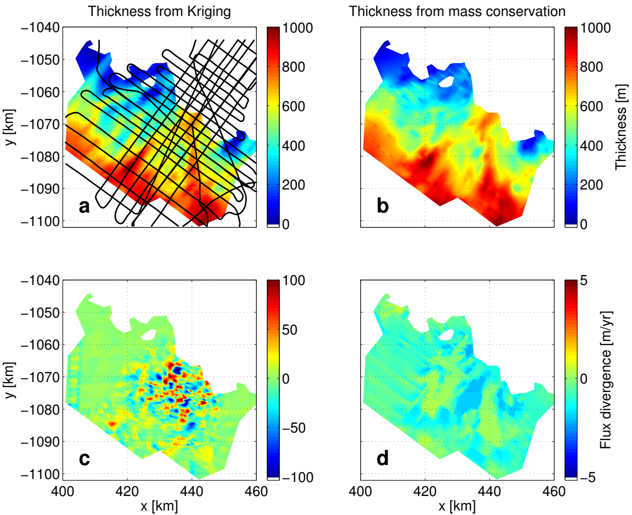

3D Hydrostatic grounding line migration

- At each time step of the transient ice flow solution, we check the following for every vertex of the mesh:

  $b \leq b_a$ where b_a is the depth of the glacier bed or seafloor. For most ice sheet/ice shelf configurations, b is negative. If this condition is verified for a floating vertex (i.e., on an ice shelf), we ground the vertex and force $b = b_a$

  $b > b_{HE}$ where b_{HE} is the depth of the bottom of the ice in hydrostatic equilibrium: $b_{HE} = H\rho/\rho_w$. If this condition is verified for a grounded vertex (i.e., on the ice sheet), we unground the vertex and force $b = b_{HE}$

3D Hydrostatic grounding line migration

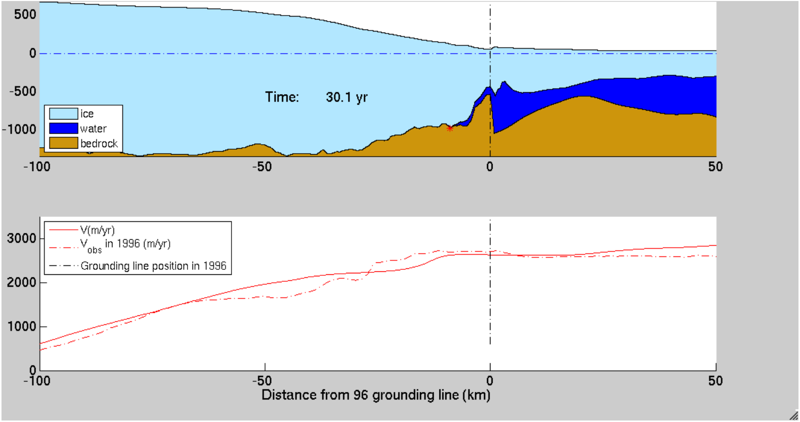

3D Hydrostatic grounding line migration

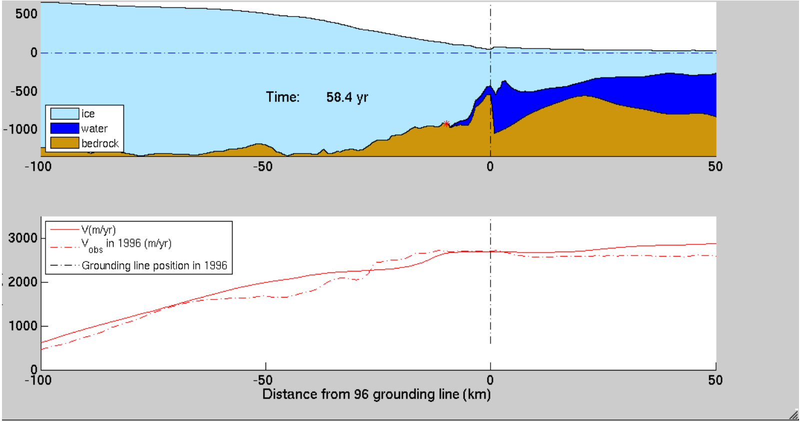

3D Hydrostatic grounding line migration

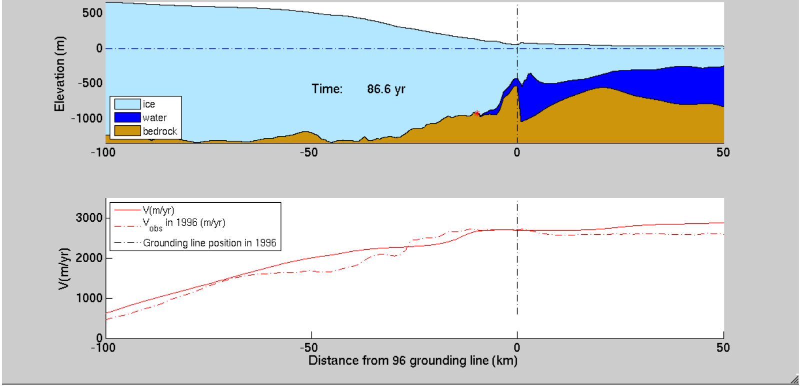

3D Hydrostatic grounding line migration

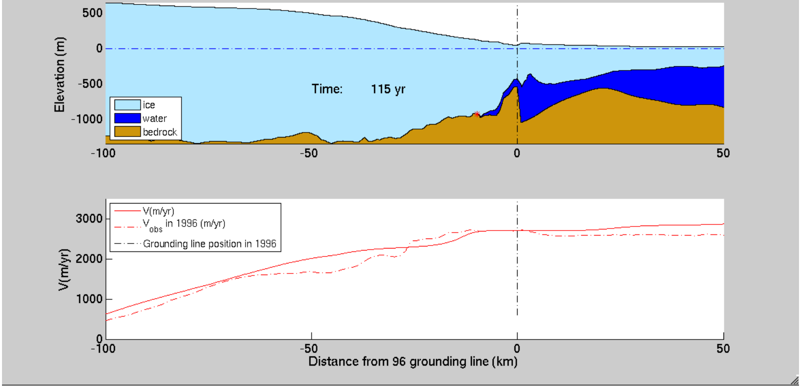

3D Hydrostatic grounding line migration

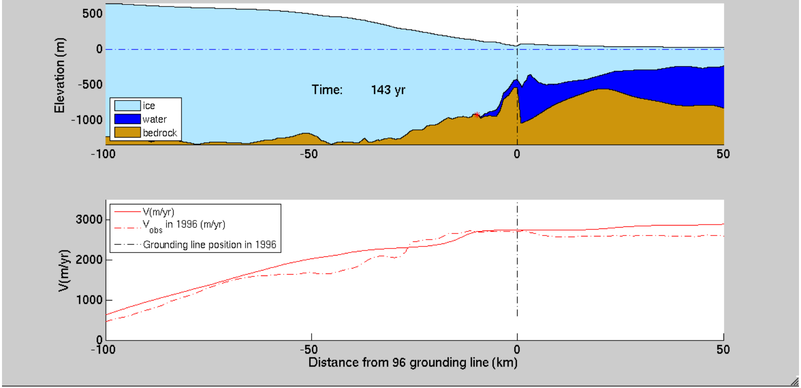

3D Hydrostatic grounding line migration

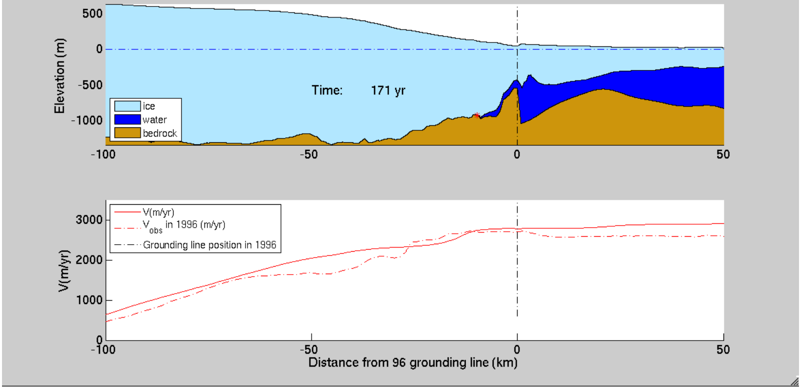

3D Hydrostatic grounding line migration

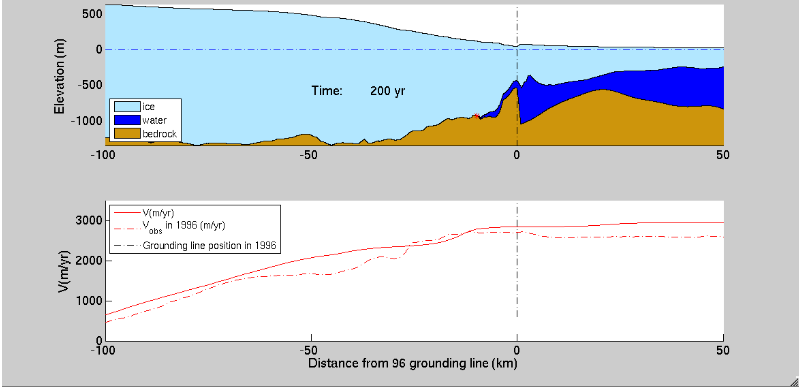

3D Hydrostatic grounding line migration

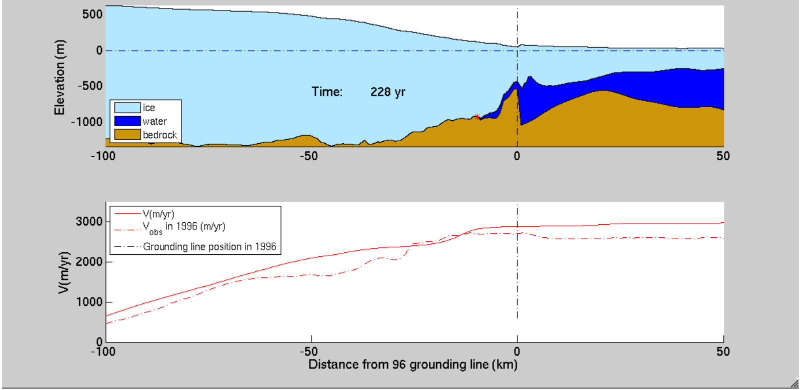

3D Hydrostatic grounding line migration

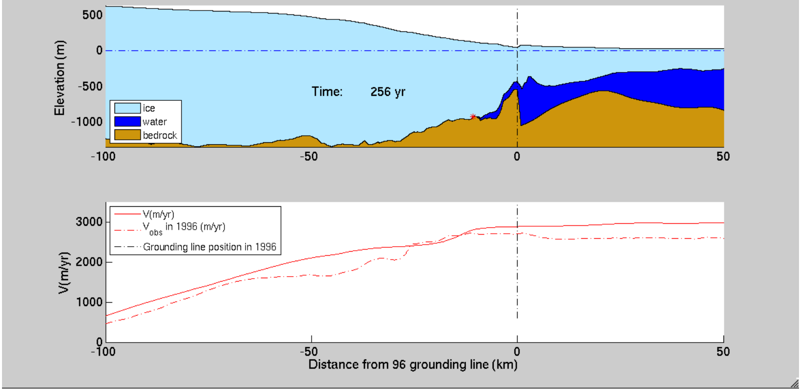

3D Hydrostatic grounding line migration

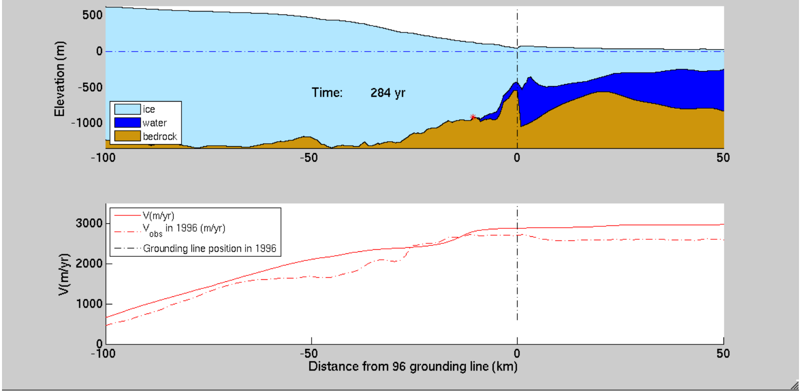

3D Hydrostatic grounding line migration

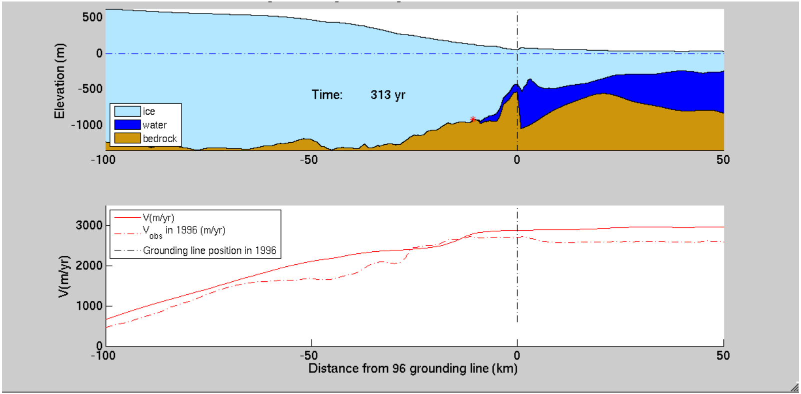

3D Hydrostatic grounding line migration

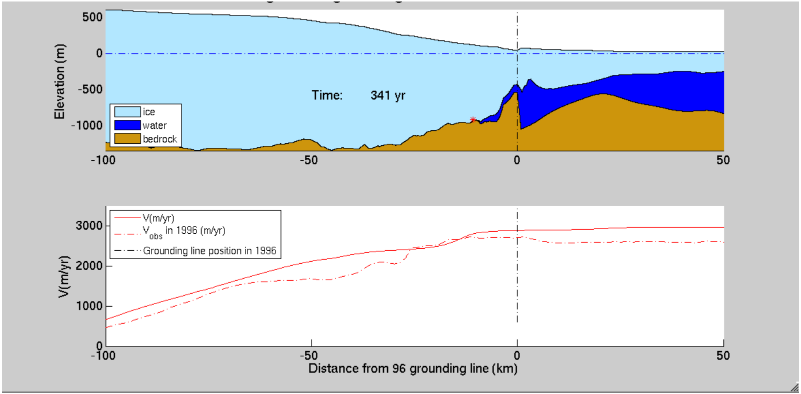

3D Hydrostatic grounding line migration

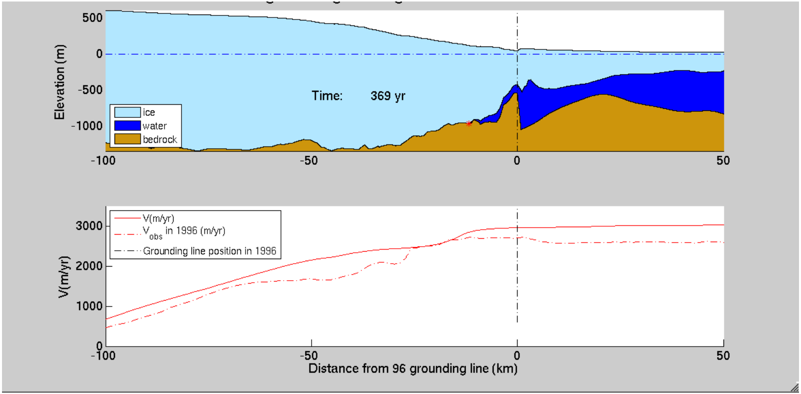

3D Hydrostatic grounding line migration

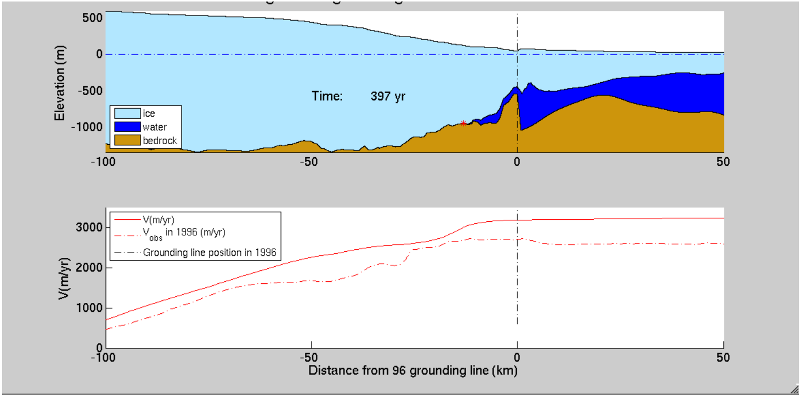

3D Hydrostatic grounding line migration

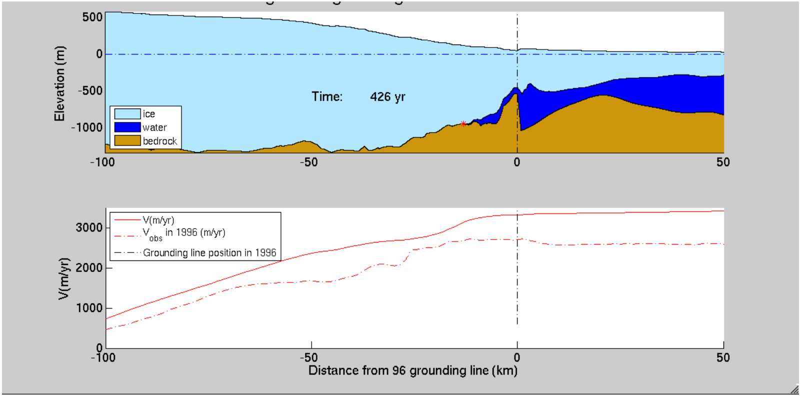

3D Hydrostatic grounding line migration

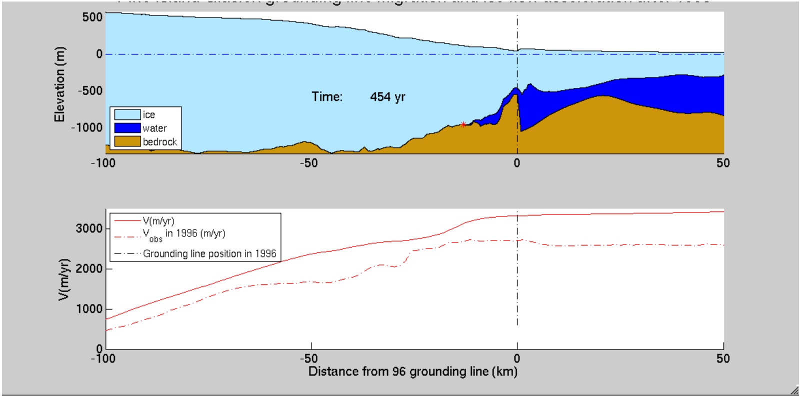

3D Hydrostatic grounding line migration

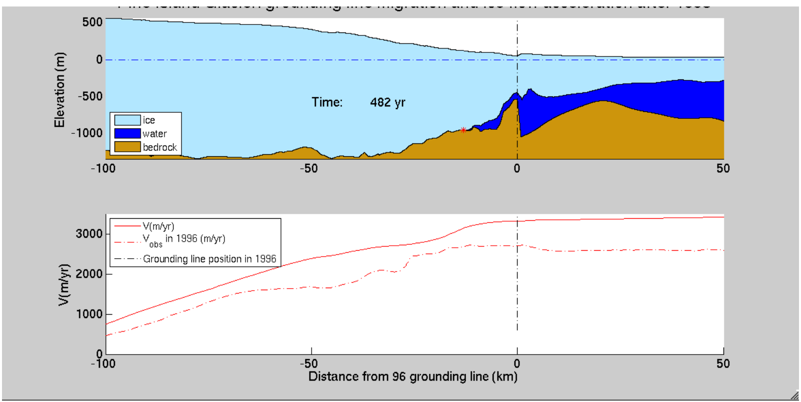

3D Hydrostatic grounding line migration

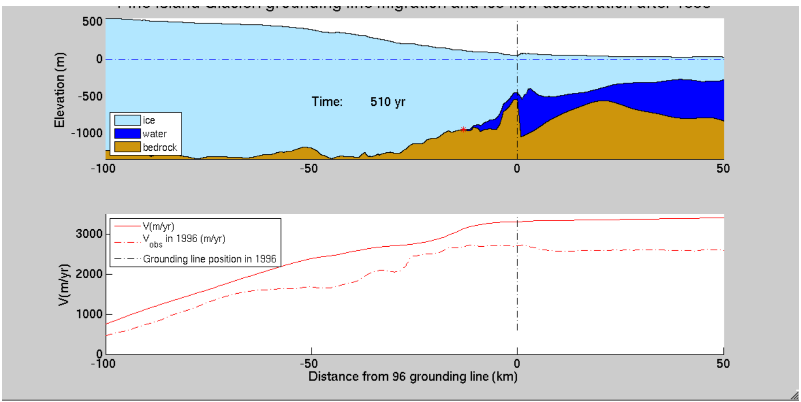

3D Hydrostatic grounding line migration

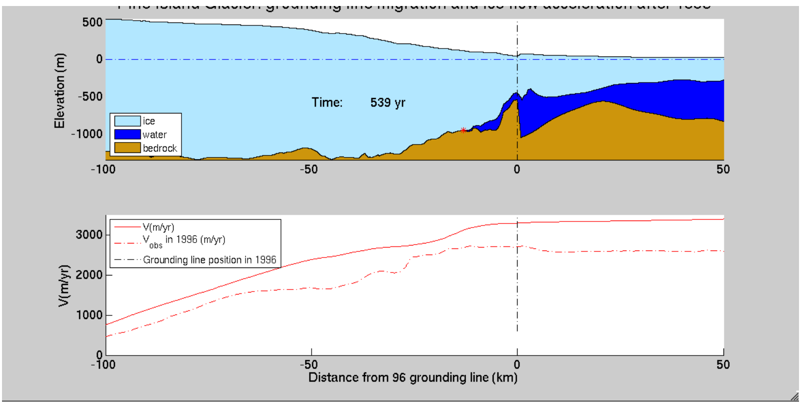

3D Hydrostatic grounding line migration

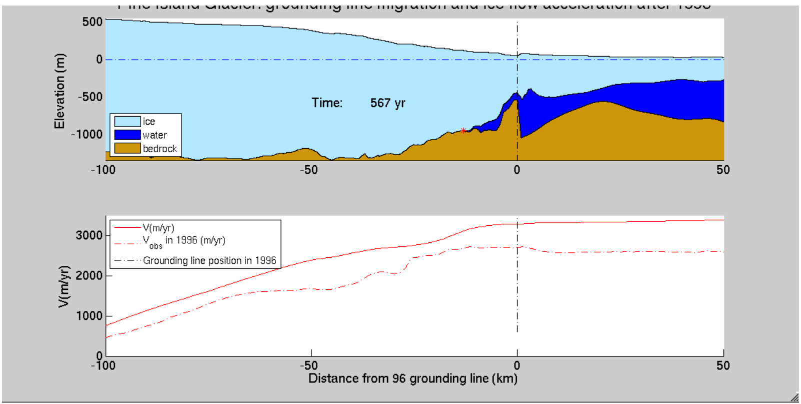

3D Hydrostatic grounding line migration

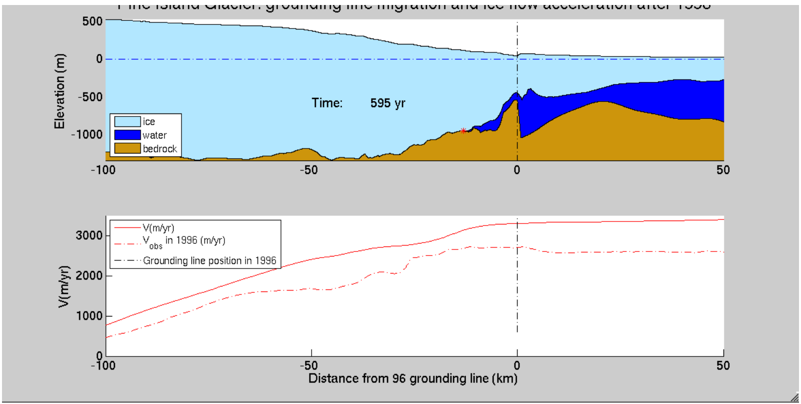

3D Hydrostatic grounding line migration

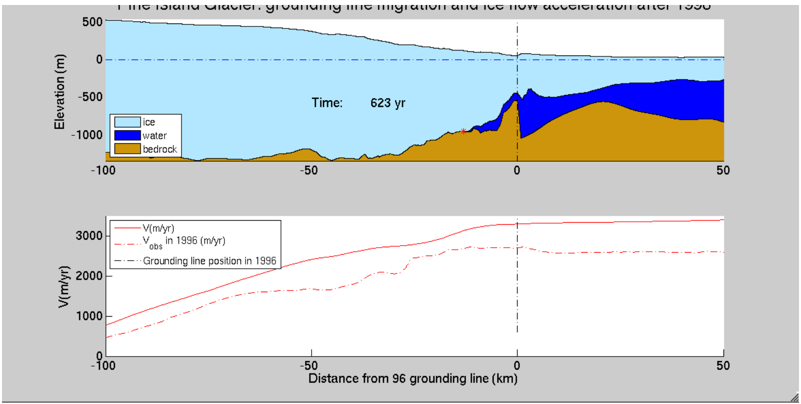

3D Hydrostatic grounding line migration

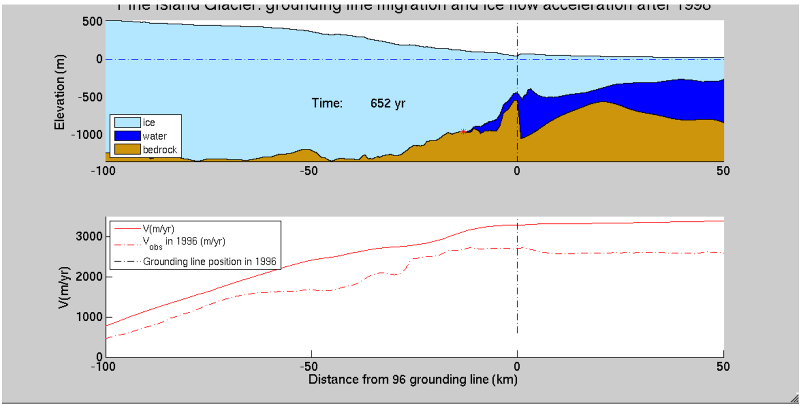

3D Hydrostatic grounding line migration

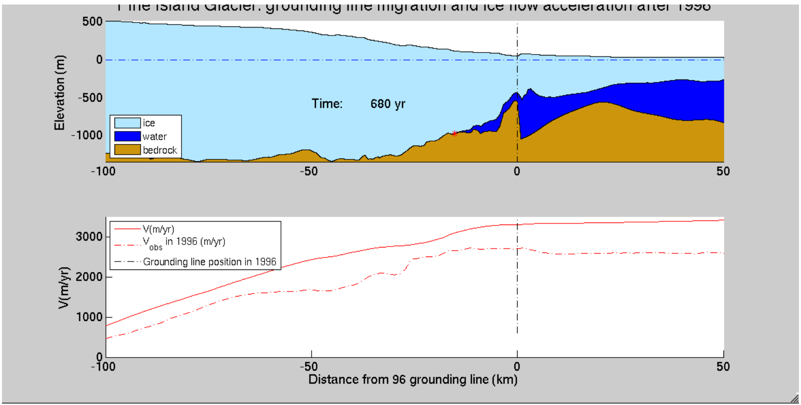

3D Hydrostatic grounding line migration

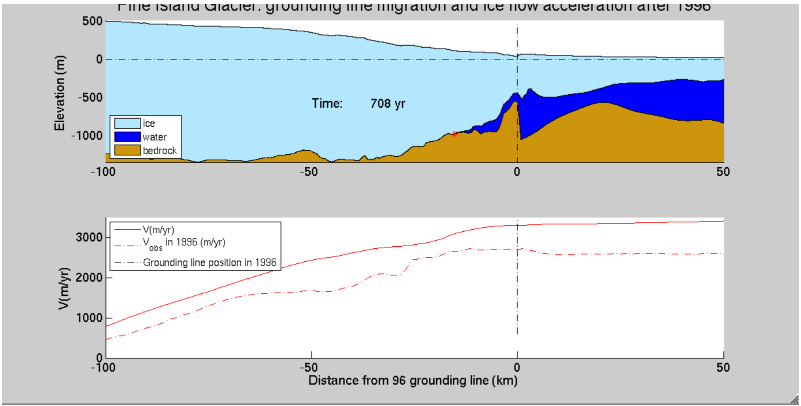

3D Hydrostatic grounding line migration

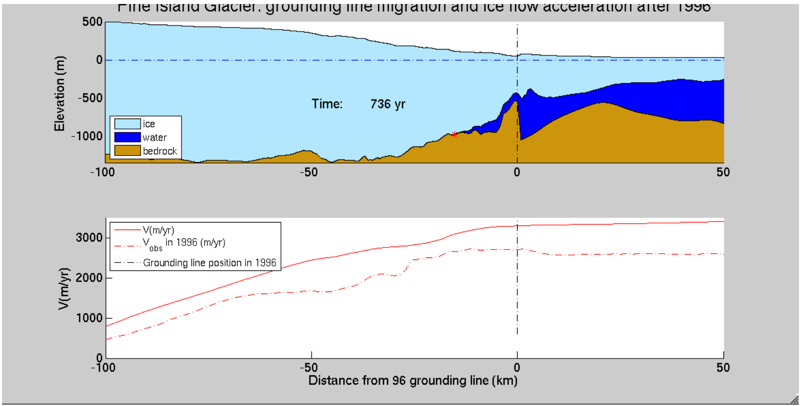

3D Hydrostatic grounding line migration

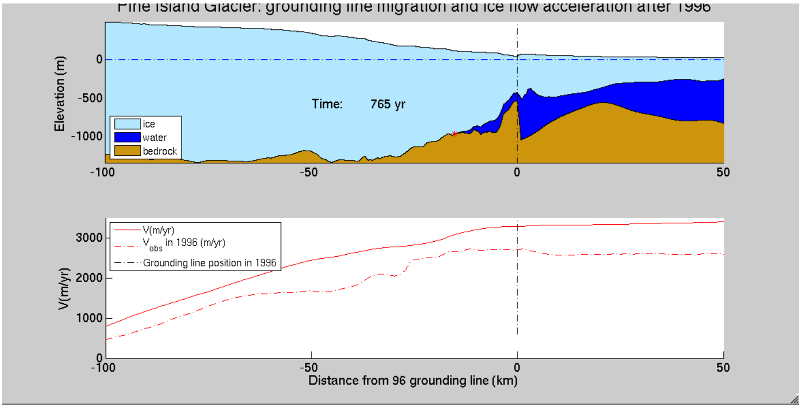

3D Hydrostatic grounding line migration

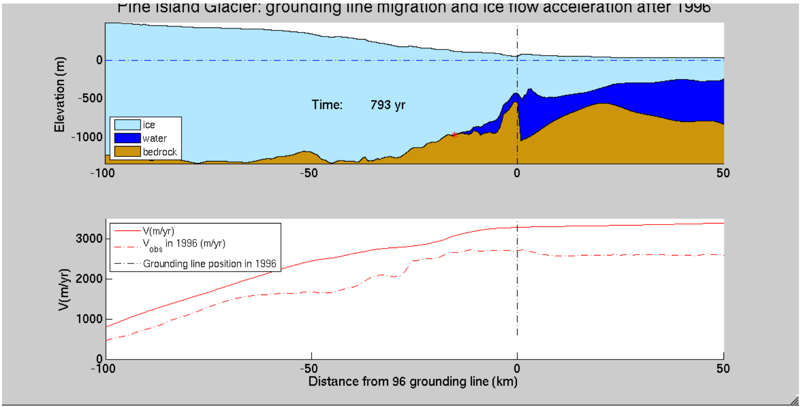

3D Hydrostatic grounding line migration

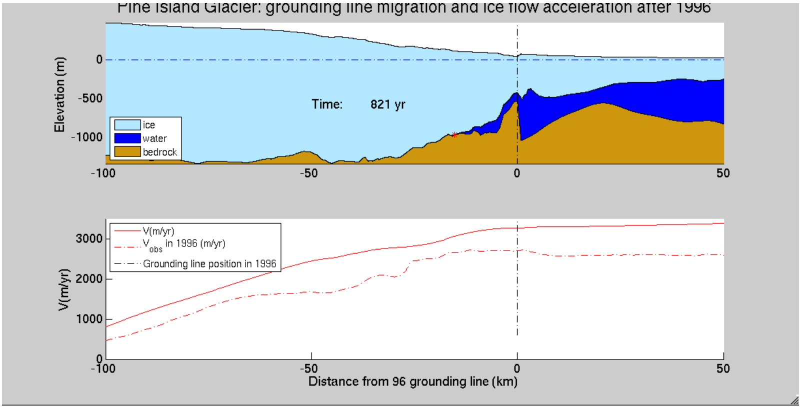

3D Hydrostatic grounding line migration

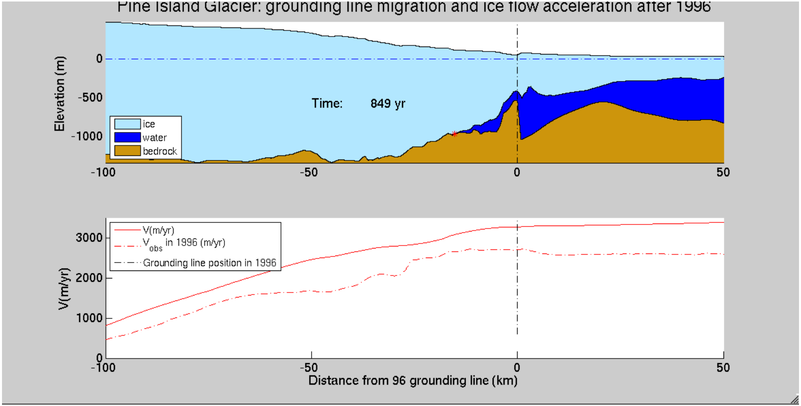

3D Hydrostatic grounding line migration

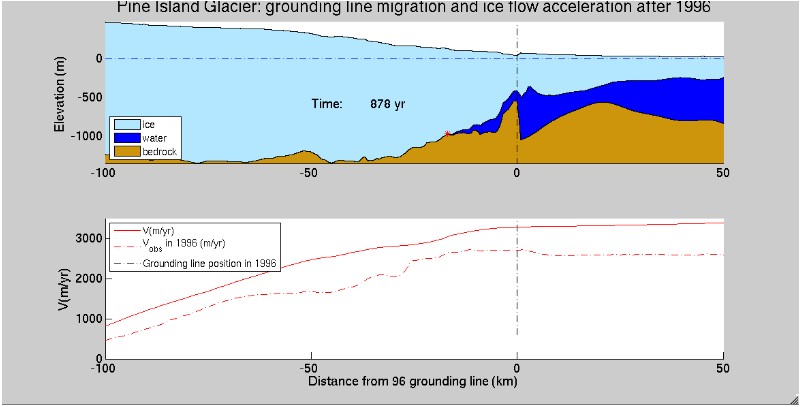

3D Hydrostatic grounding line migration

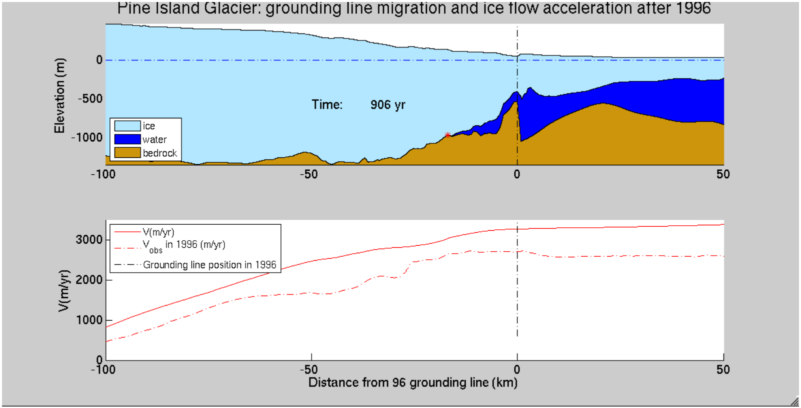

3D Hydrostatic grounding line migration

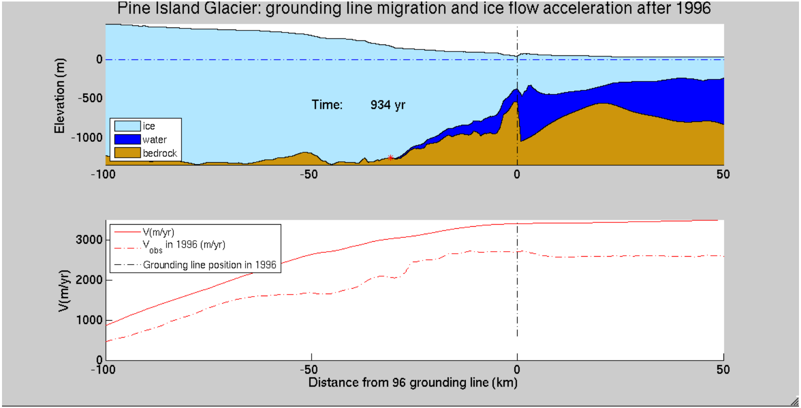

3D Hydrostatic grounding line migration

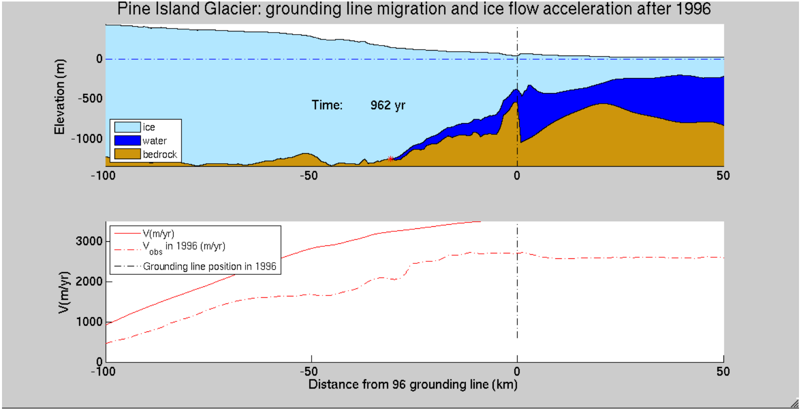

3D Hydrostatic grounding line migration

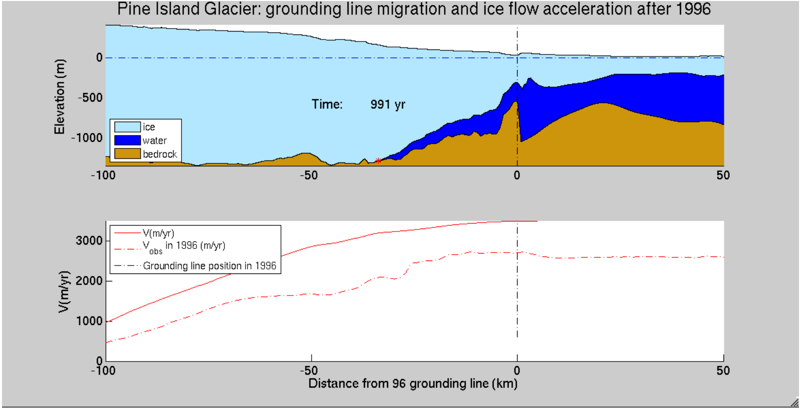

3D Hydrostatic grounding line migration

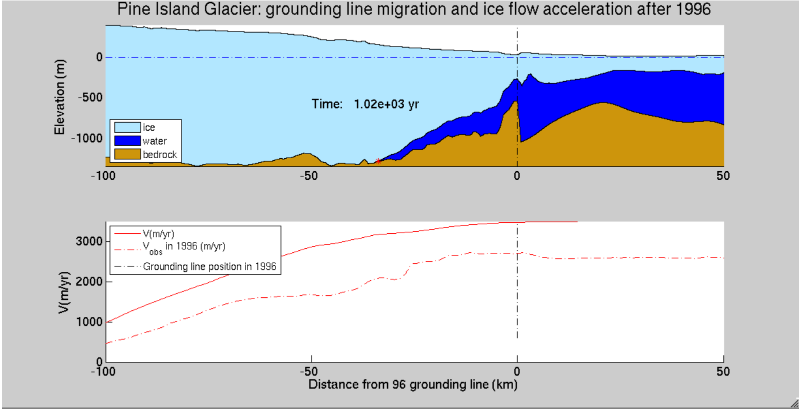

3D Hydrostatic grounding line migration

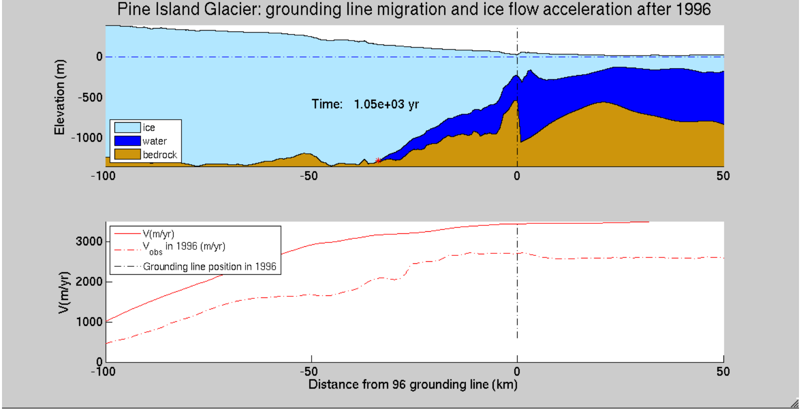

3D Hydrostatic grounding line migration

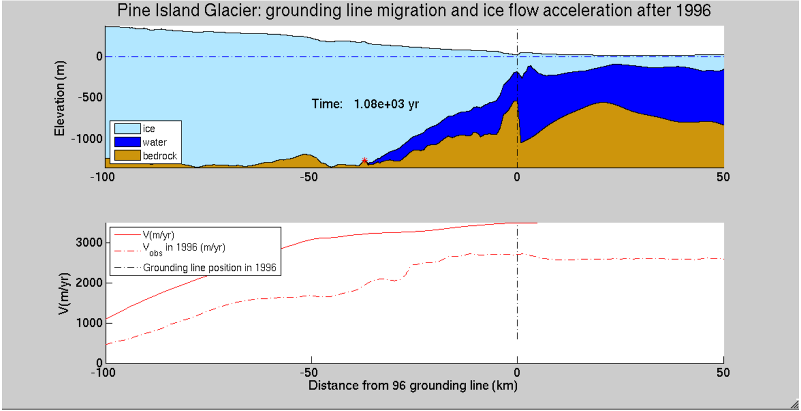

3D Hydrostatic grounding line migration

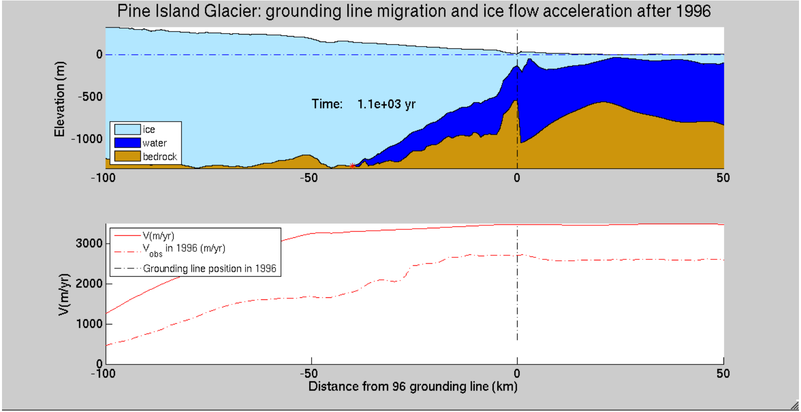

3D Hydrostatic grounding line migration

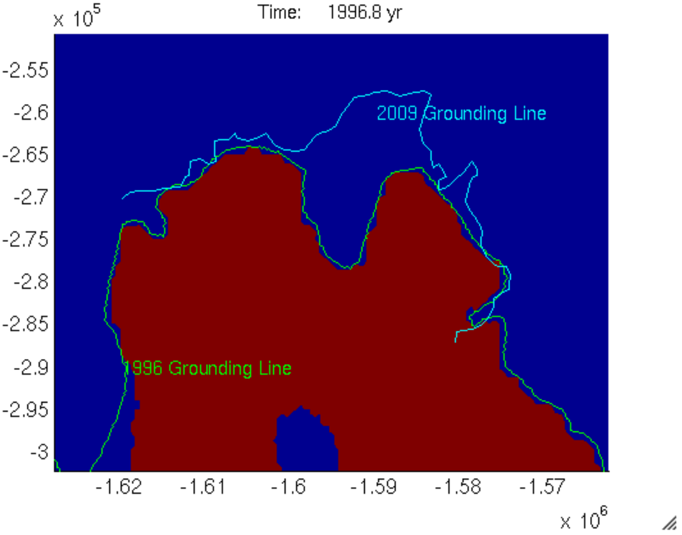

3D Hydrostatic grounding line migration

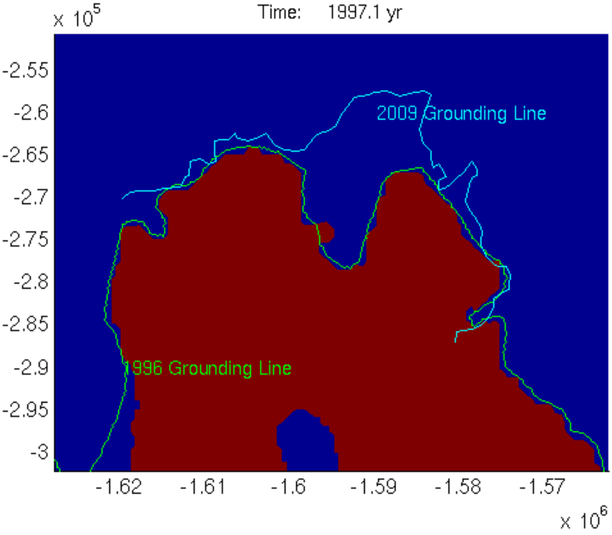

3D Hydrostatic grounding line migration

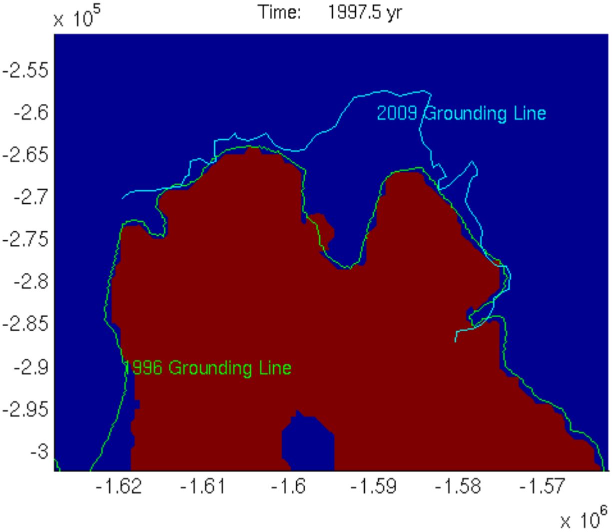

Capabilities
Larour et al.
Introduction
Diagnostic Models
Inversion
Parallel Computing
Rifting/Faulting
Higher-order, Full-Stokes
Anisotropic Adaptation
Prognostic Models
Thermal Analysis
Sensitivity Analysis
Ice Thickness Assimilation
3D Hydrostatic Grounding Line Migration
Hydrology
Svn/Trac
Nightly Runs
Test Suite
Doxygen
Conclusions

3D Hydrostatic grounding line migration

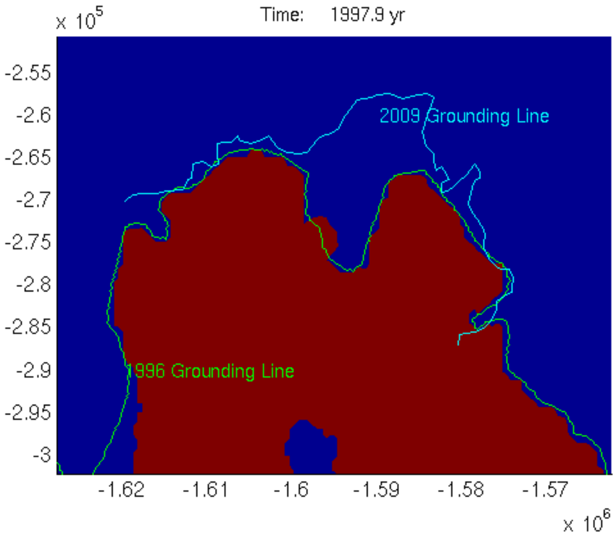

3D Hydrostatic grounding line migration

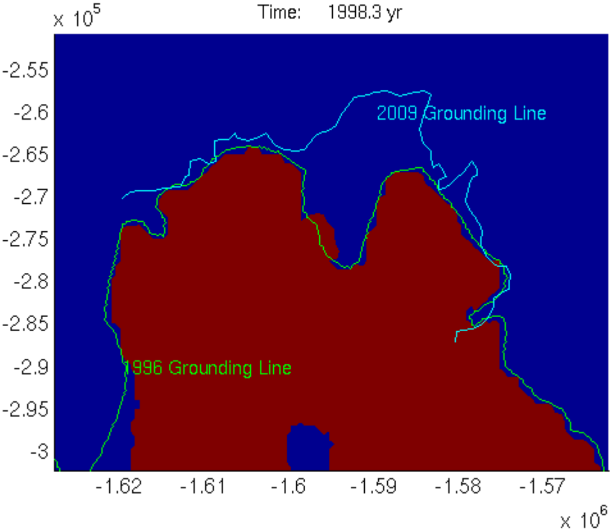

3D Hydrostatic grounding line migration

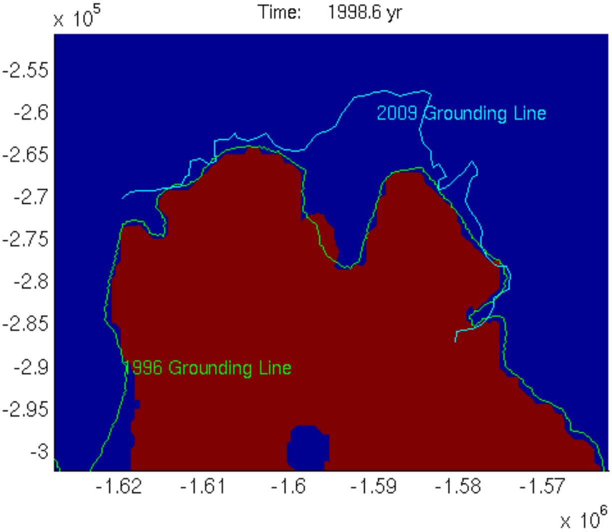

3D Hydrostatic grounding line migration

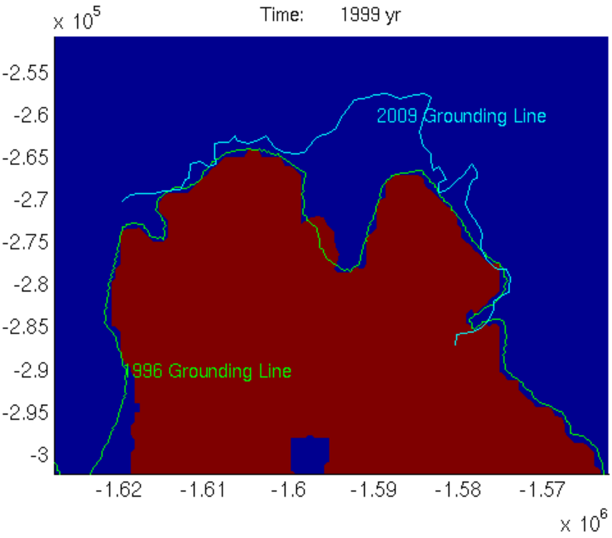

3D Hydrostatic grounding line migration

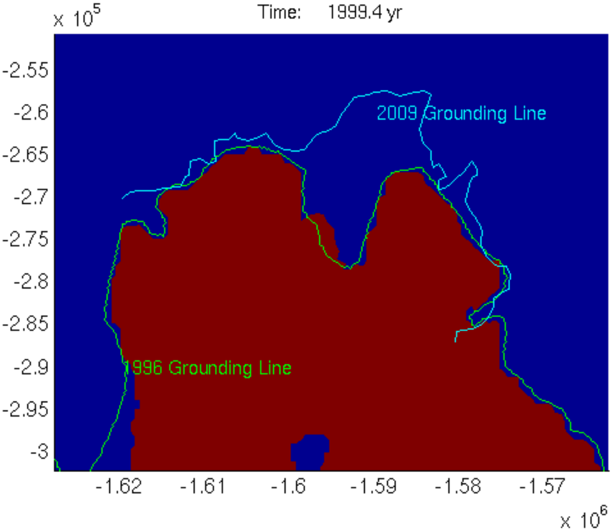

3D Hydrostatic grounding line migration

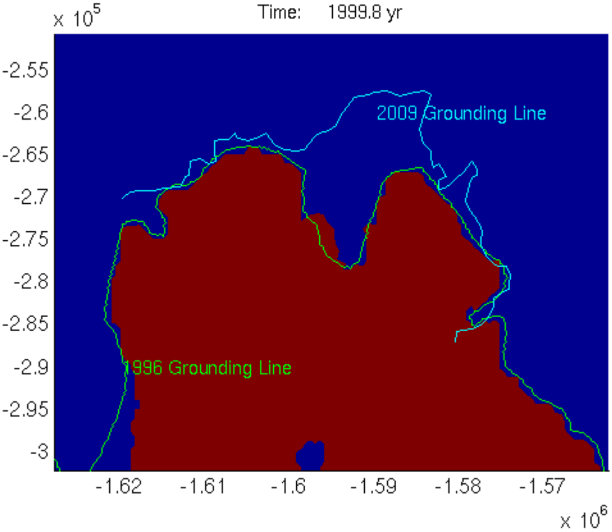

3D Hydrostatic grounding line migration

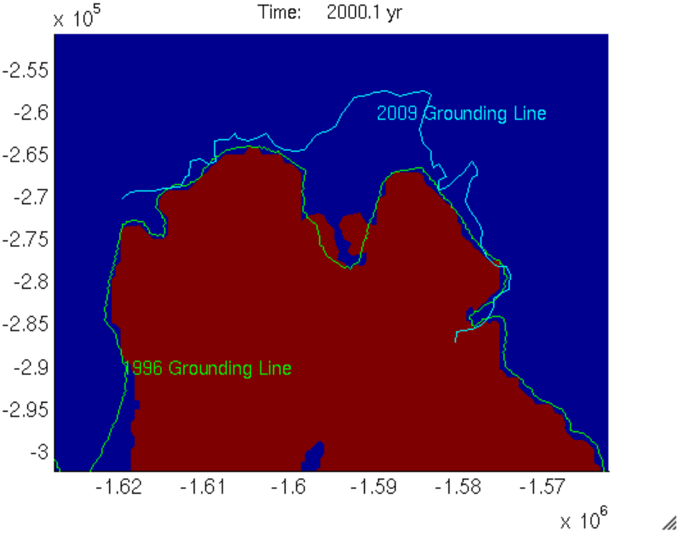

3D Hydrostatic grounding line migration

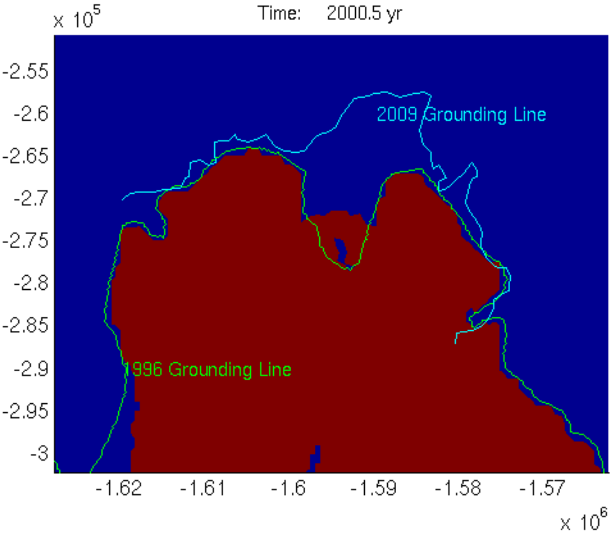

3D Hydrostatic grounding line migration

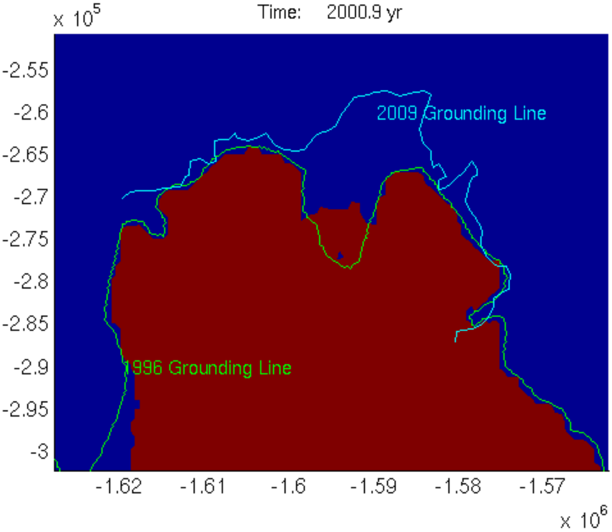

3D Hydrostatic grounding line migration

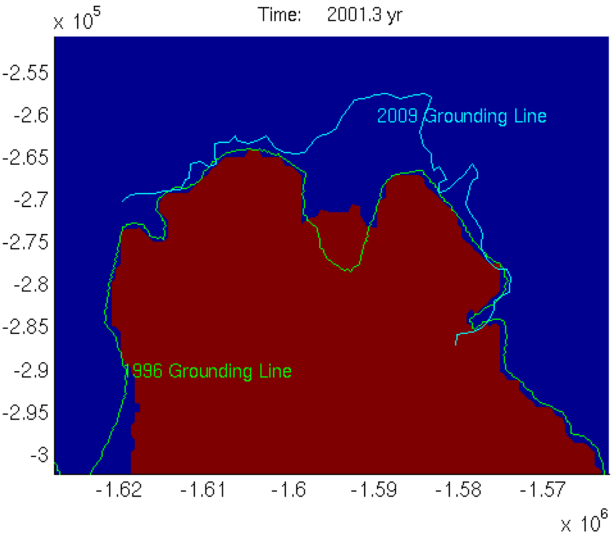

3D Hydrostatic grounding line migration

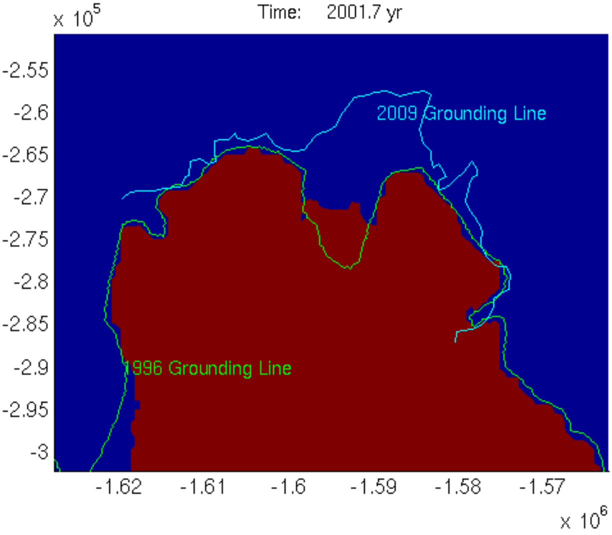

3D Hydrostatic grounding line migration

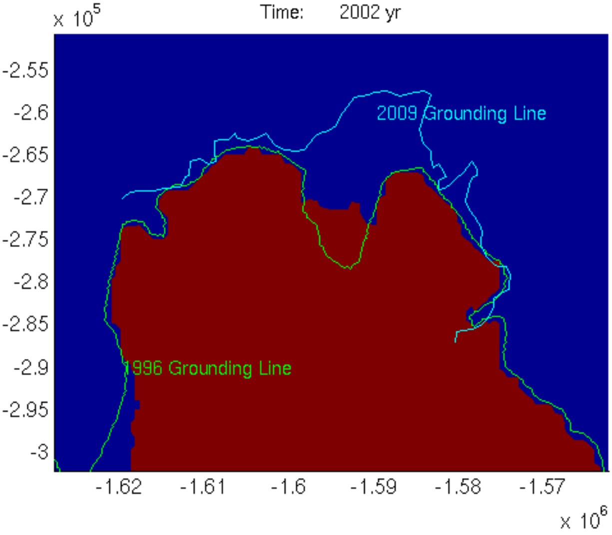

3D Hydrostatic grounding line migration

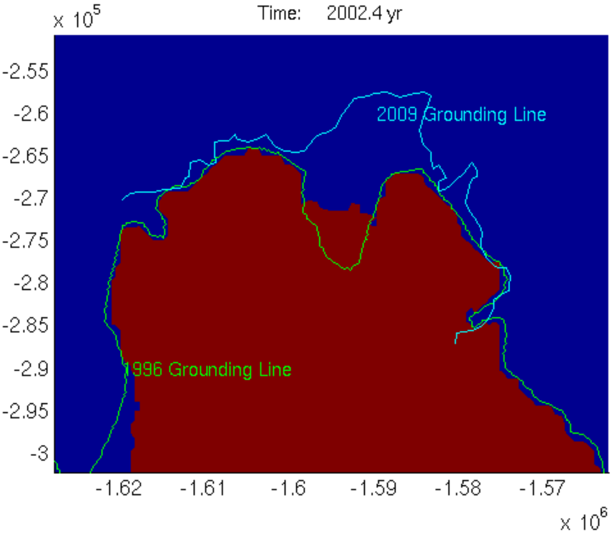

3D Hydrostatic grounding line migration

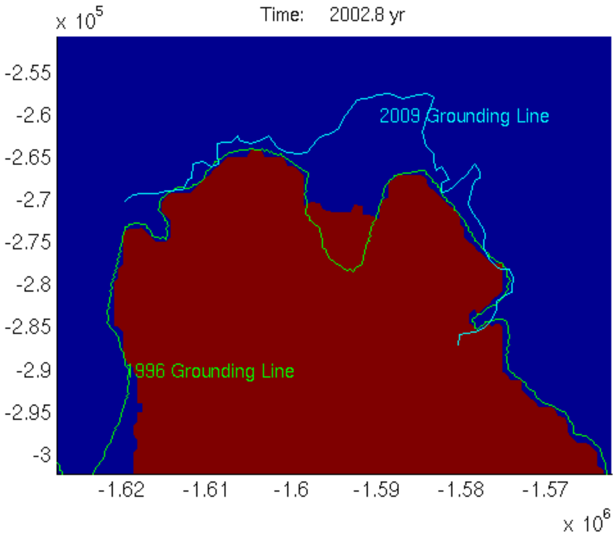

3D Hydrostatic grounding line migration

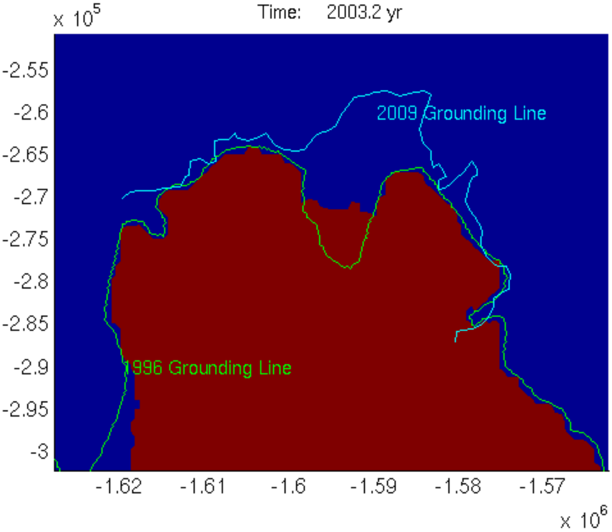

3D Hydrostatic grounding line migration

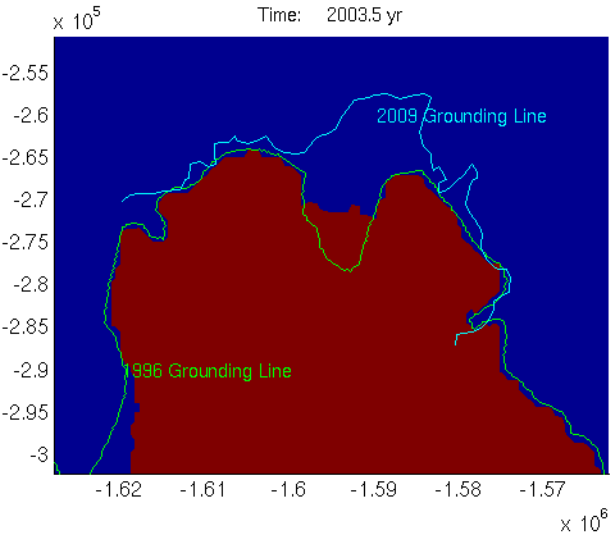

3D Hydrostatic grounding line migration

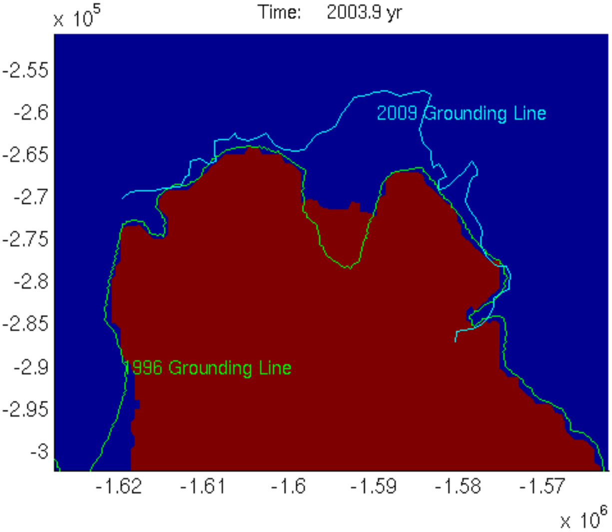

3D Hydrostatic grounding line migration

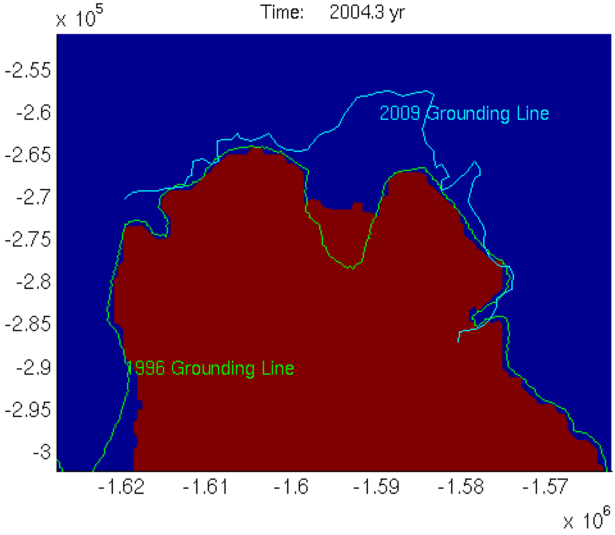

3D Hydrostatic grounding line migration

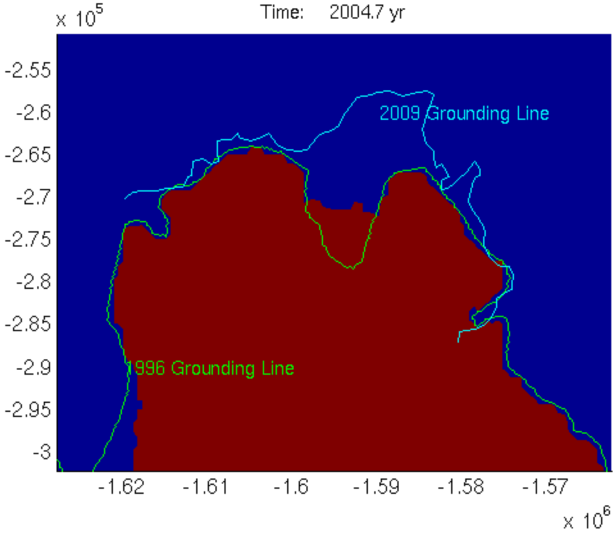

3D Hydrostatic grounding line migration

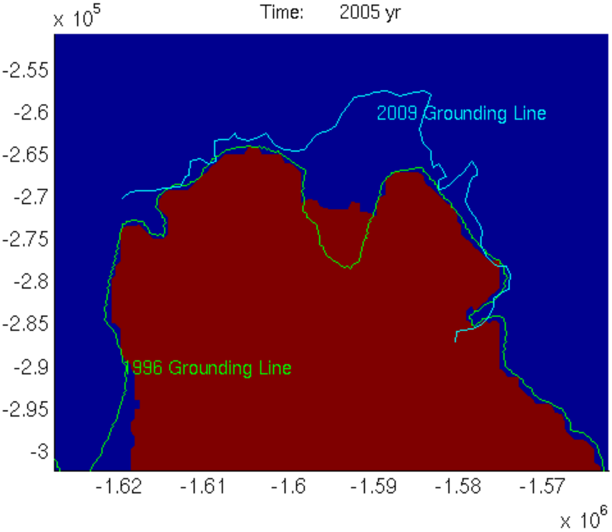

3D Hydrostatic grounding line migration

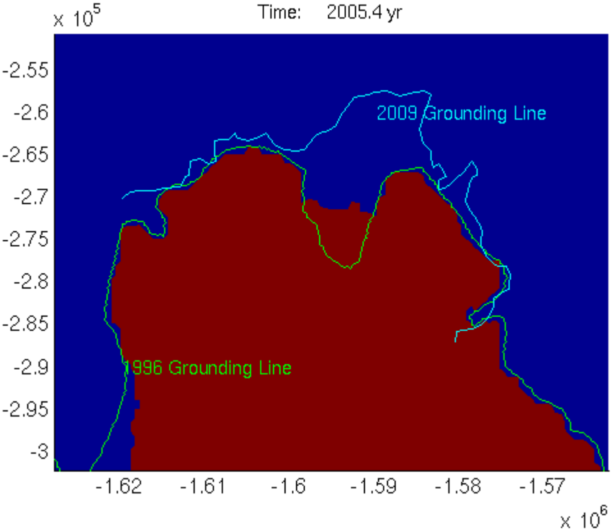

3D Hydrostatic grounding line migration

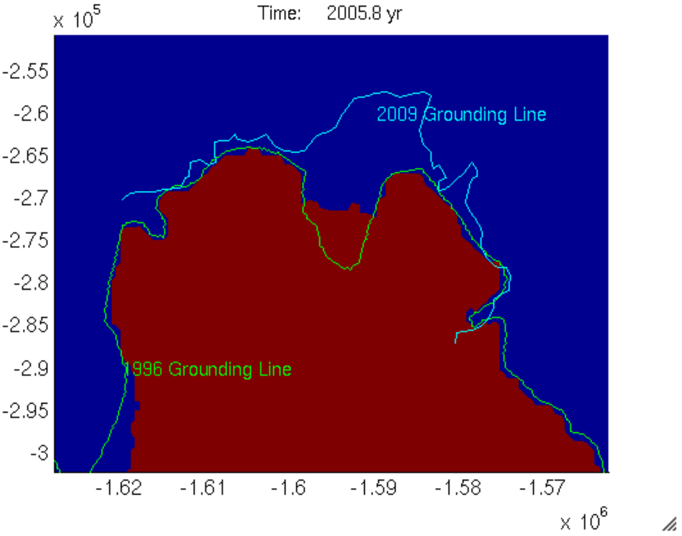

3D Hydrostatic grounding line migration

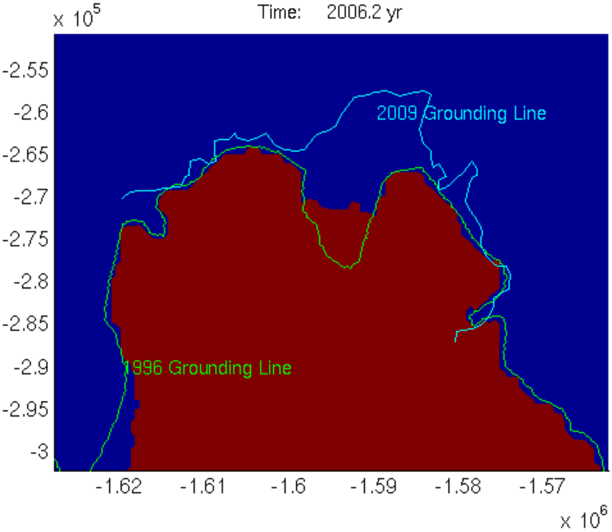

3D Hydrostatic grounding line migration

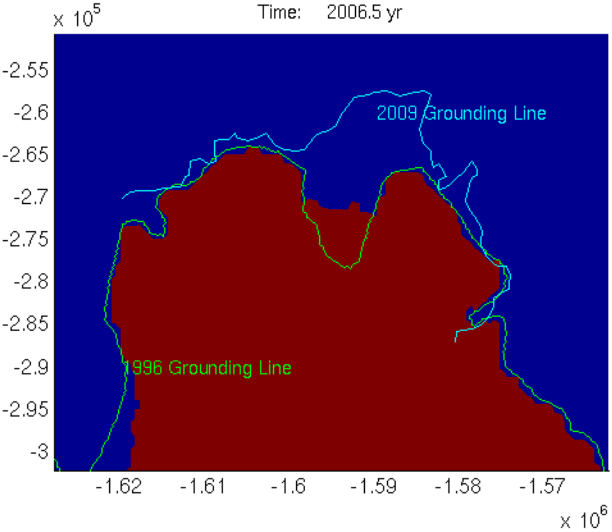

3D Hydrostatic grounding line migration

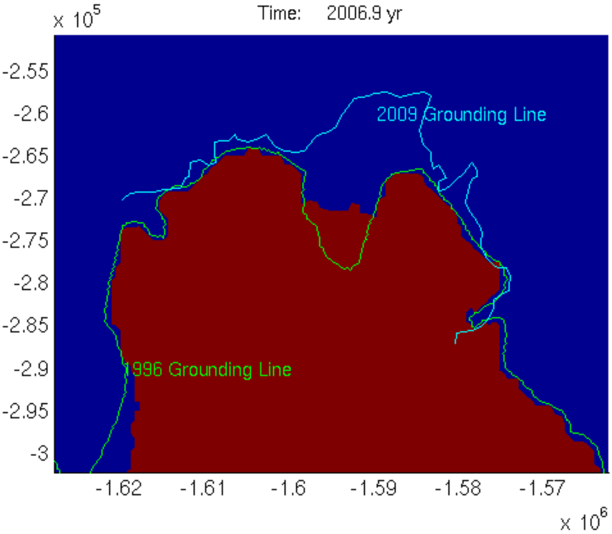

3D Hydrostatic grounding line migration

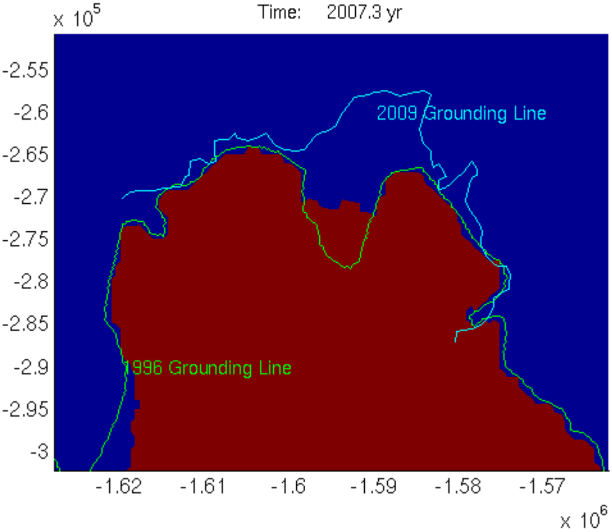

3D Hydrostatic grounding line migration

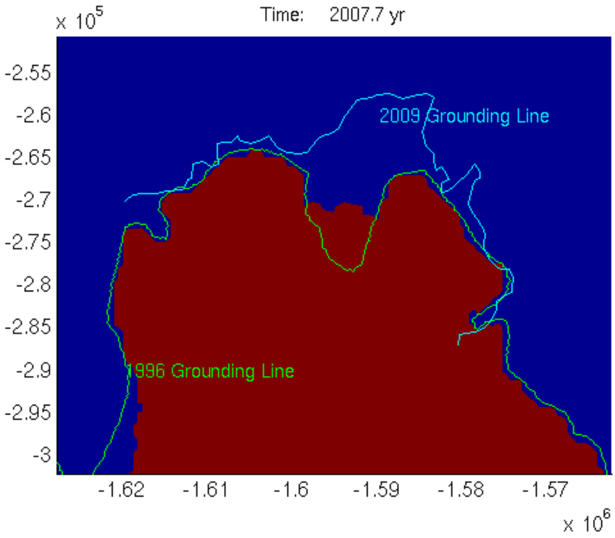

3D Hydrostatic grounding line migration

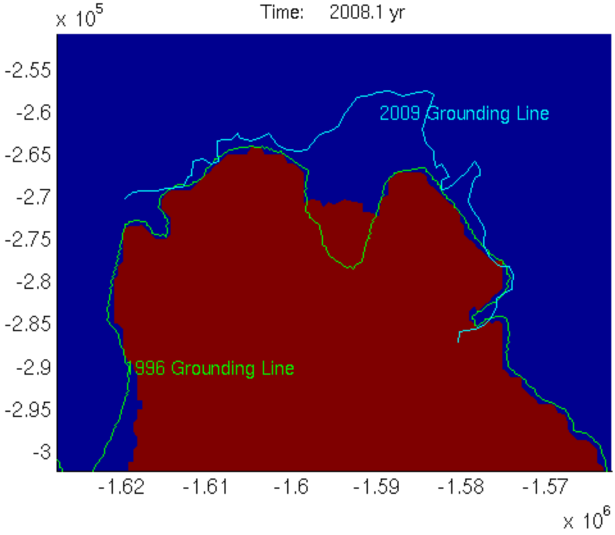

3D Hydrostatic grounding line migration

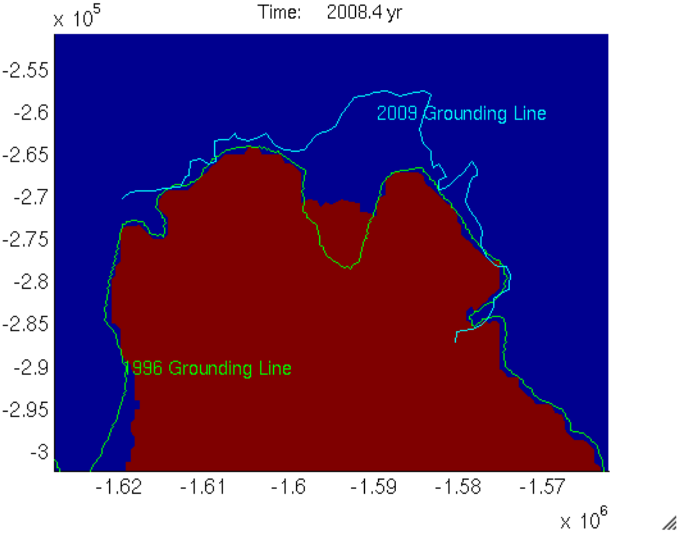

3D Hydrostatic grounding line migration

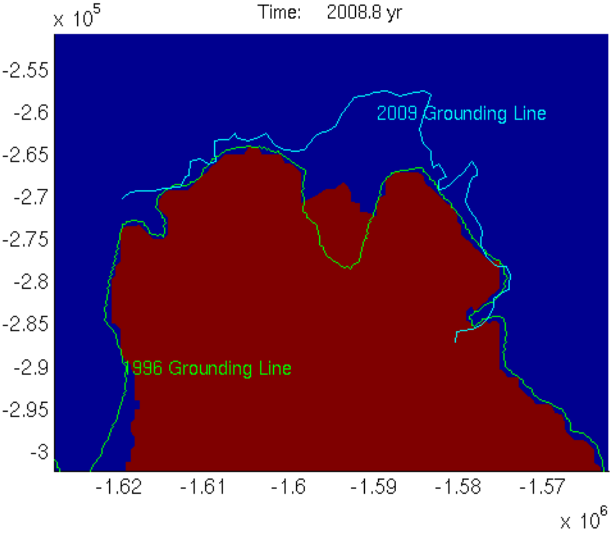

3D Hydrostatic grounding line migration

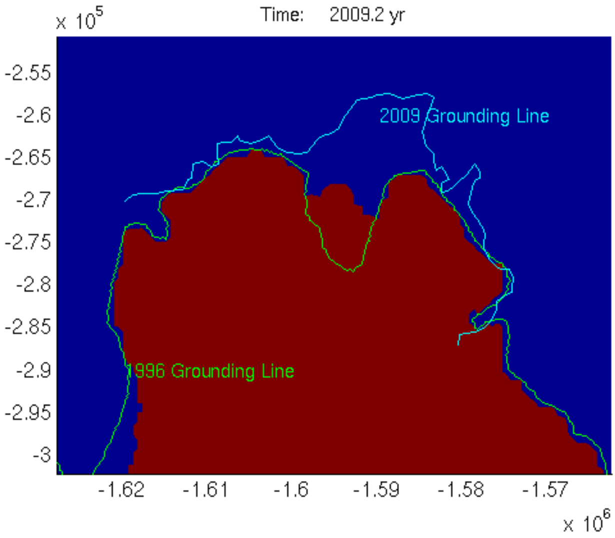

3D Hydrostatic grounding line migration

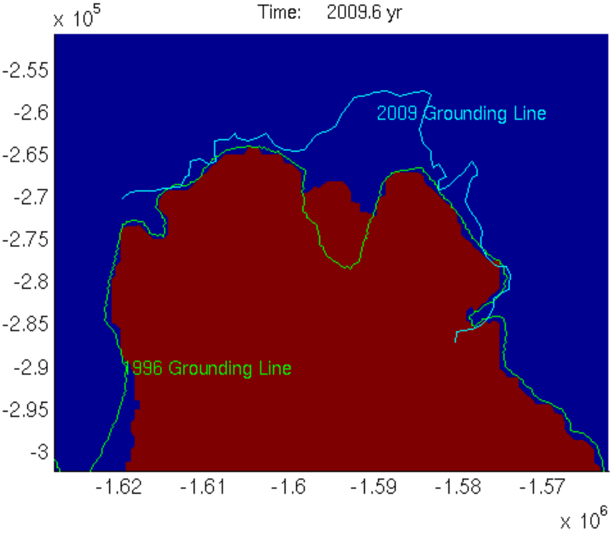

3D Hydrostatic grounding line migration

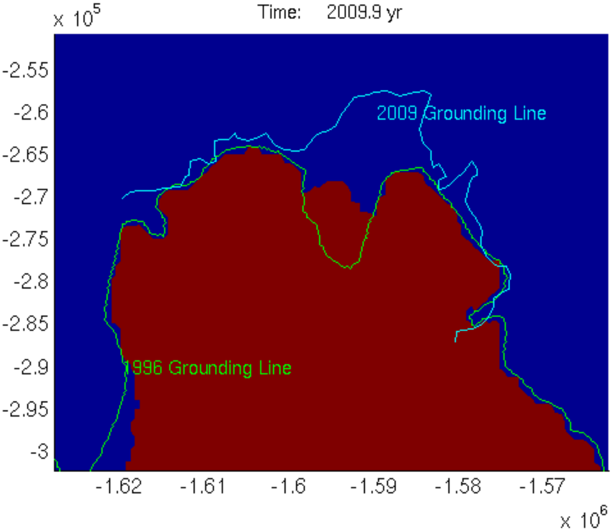

3D Hydrostatic grounding line migration

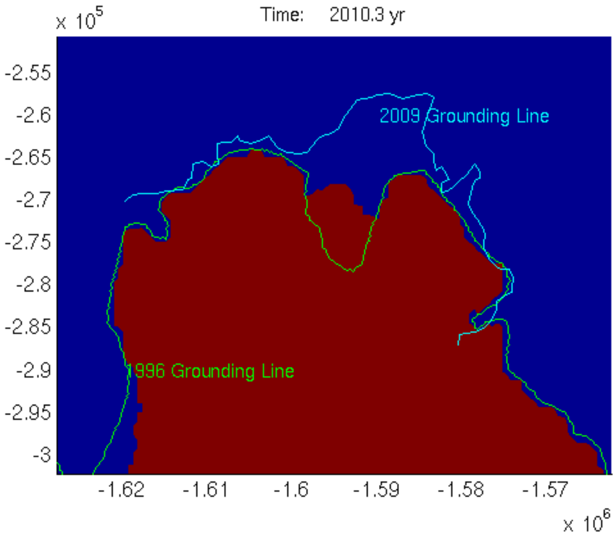

3D Hydrostatic grounding line migration

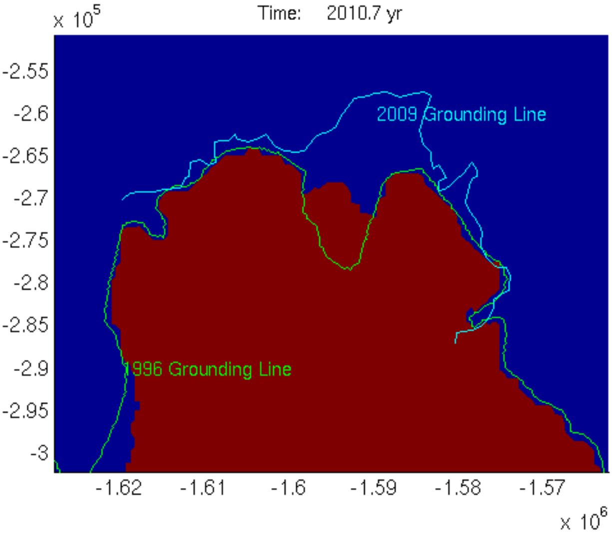

Hydrology model

[Le Brocq et al., 2009]: the evolution of the water-film thickness (w) is given by:

$$\frac{dw}{dt} = S - \nabla.(w.\overline{u_w})$$

With w the water thickness, S the basal melting rate and $\bar{u_w}$ the depth-averaged water velocity vector.
Assuming a laminar flow between two parallel plates:

$$\overline{u_w} = \frac{w^2 \nabla \Phi}{12\mu} \quad \text{and} \quad \Phi = \rho_i g z_s + (\rho_w - \rho_i) g z_b - N$$

where μ is the water viscosity, z_s and z_b the surface and bed elevatinos, N the effective pressure and Φ the pressure potential.

Hydrology model

Because we assume a non-arborescent drainage system, we cancel the effective pressure *N*:

$$\nabla\Phi = \rho_i g \nabla z_s + (\rho_w - \rho_i) g \nabla z_b$$

This set of assumptions results in the following non-linear system:

$$\frac{dw}{dt} = S - \nabla . \left(\frac{w^3}{12\mu} \nabla\Phi \right)$$

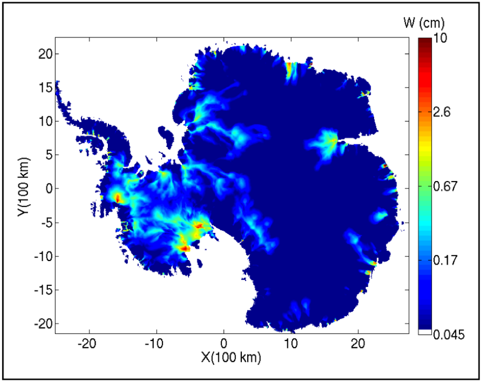

Svn/Trac

Download page:

`http://issm.jpl.nasa.gov/installation/download/`

- Install SVN (Apache Subversion)
- Checkout ISSM:

  ```
  $ svn –username anon –password anon checkout
  https://issm.ess.uci.edu:80/svn/issm/issm
  ```
- Update ISSM:

  ```
  $ svn update
  ```

Capabilities

Larour et al.

Svn/Trac

Trac system with wiki

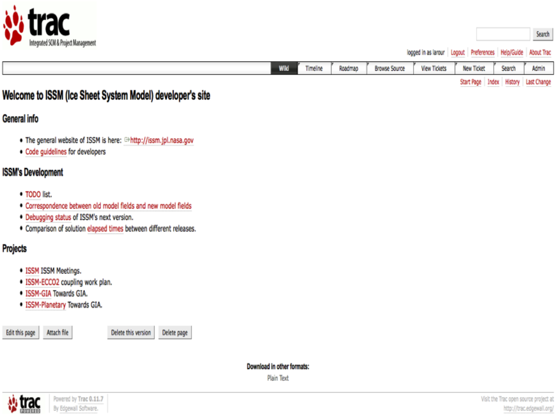

Nightly runs

ISSM Nightly run report

host: larsen	date: Dec-10-2011 23:00:01
OS: astrid	user: seroussi
status: all test desks have been run	release: trunk-jpl
number of successes: 2511/2658	total elapsed time: 10:03:27
number of errors: 141/2658	installation elapsed time: 3:19:25
number of failures: 6/2658	execution elapsed time: 6:44:02

List of tests

Result	Tolerance	Test id	Test name	Field checked
SUCCESS	3.3e-15<1e-13	101	SquareShelfConstrainedDiagM2dSerial	Vx
SUCCESS	1.9e-15<1e-13	101	SquareShelfConstrainedDiagM2dSerial	Vy
SUCCESS	2e-15<1e-13	101	SquareShelfConstrainedDiagM2dSerial	Vel
SUCCESS	1e-16<1e-13	101	SquareShelfConstrainedDiagM2dSerial	Pressure
SUCCESS	3.4e-15<1e-13	102	SquareShelfConstrainedDiagM2dParallel	Vx
SUCCESS	1.3e-15<1e-13	102	SquareShelfConstrainedDiagM2dParallel	Vy
SUCCESS	1.3e-15<1e-13	102	SquareShelfConstrainedDiagM2dParallel	Vel
SUCCESS	1e-16<1e-13	102	SquareShelfConstrainedDiagM2dParallel	Pressure
SUCCESS	2.1e-15<1e-13	103	SquareShelfConstrainedDiagM3dSerial	Vx
SUCCESS	9.4e-16<1e-13	103	SquareShelfConstrainedDiagM3dSerial	Vy
SUCCESS	5.3e-16<1e-13	103	SquareShelfConstrainedDiagM3dSerial	Vz
SUCCESS	1.4e-15<1e-13	103	SquareShelfConstrainedDiagM3dSerial	Vel
SUCCESS	0<1e-13	103	SquareShelfConstrainedDiagM3dSerial	Pressure
SUCCESS	3e-15<1e-13	104	SquareShelfConstrainedDiagM3dParallel	Vx
SUCCESS	1.1e-15<1e-13	104	SquareShelfConstrainedDiagM3dParallel	Vy

Test suite

- 626 tests run on a nightly-basis
- Serial/Parallel run comparisons
- Internal checks
- Solution checks
- Numerical accuracy checks
- Run several times a day, to capture code updates which break the software

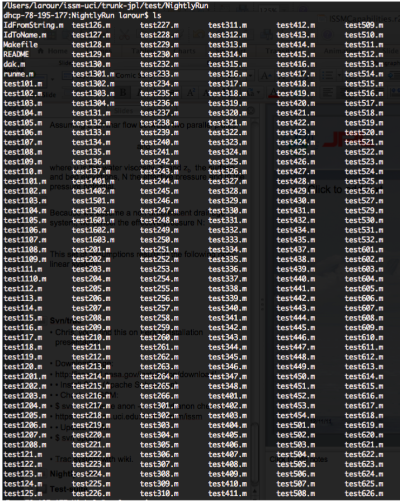

Doxygen

Ice Sheet System Model 3.3

C/C++ code documentation

Main Page | Data Structures | Files | Directories

ISSM C/C++ Source Code Browser

Welcome !

This is the searchable browsing tool for ISSM (the Ice Sheet System Model).

These pages were automatically generated by doxygen, from comments in the ISSM source code.

Navigate the tabs above and browse through ISSM's C++ source code, files/directories, and data structures.

To find additional information regarding the use of ISSM, its current release, or the ISSM team, please visit http://issm.jpl.nasa.gov.

Helpful Links

- Fill out an ISSM download request here.
- ISSM Installation instructions are found here.
- For help using ISSM, see our online User's Manual. Other documentation is also available including simple tutorials and FAQ.
- A current publication list is kept here.
- Contact us by e-mail at issm@jpl.nasa.gov

Code Stats

Language	files	blank	comment	code	Total
C++	531	15433	17169	57344	89946
MATLAB	970	7248	13716	31608	52572
C/C++ Header	397	3047	2706	10262	16015
Objective C	32	99	0	402	501
Bourne Shell	9	59	98	272	429
Perl	3	21	23	240	284

Conclusions

- ISSM represents a wide array of capabilities, geared toward solving specific cryosphere challenges such as projections of future sea level rise
- Extensive software and architecture support, as well as wide array of numerical solutions and physics implemented
- Challenges remain, such as grounding line dynamics using FS, moving margins and ice/ocean interactions

Bibliography I

Hecht, F. (2006).
BAMG: Bi-dimensional anisotropic mesh generator.
Technical report, FreeFem++.

Holland, D. and Jenkins, A. (1999).
Modeling thermodynamic ice-ocean interactions at the base of an ice shelf.
J. Phys. Oceanogr., 29(8, Part 1):1787–1800.

Le Brocq, A., Payne, A., Siegert, M., and Alley, R. (2009).
A subglacial water-flow model for west antarctica.
J. Glaciol., 55(193):879–888.


Thanks!